

Supplementary Materials

- I. Experimental settings of radiomic features extraction**
- II. Parameters setting of the Random Forest prediction model**
- III. Comparison of Skewness features with our selected features**
- IV. Influence of intra- and inter-observer variability on prediction**
- V. References**

Experimental settings of radiomic features extraction

Table 1 lists the radiomics features we extracted from the original PET and CT images, while the 22 GLCM features were only extracted from CT images. The definitions of these features were compliant with the Image Biomarker Standardisation Initiative [1].

In addition to features from original PET and CT images, we also extracted the same set of radiomics features respectively from the LoG and wavelet filtered images of both PET and CT images. The LoG filters were applied with three levels, i.e. $\sigma=1\text{mm}$, 3mm and 5mm , capturing three different levels of texture details. The wavelet filters could yield 8 decomposed images by applying all possible combinations of high or low pass filter in each of the three dimensions. The **Figure 1** shows the distribution of all radiomics features after feature extraction, and the detailed parameters settings for these radiomics feature extraction could be found in **Table 2**.

Table 1. The full list of extracted radiomic features.

Intensity histogram(18)	Morphology(13)	GLCM(22)	GLRLM(16)	GLSZM(16)	NGTDM(14)
10percentile	Elongation	AutoCorrelation	GLNU	GLNU	DependenceEntropy
90Percentile	Flatness	ClusterProminence	GLNUN	GLNUN	DNU
Energy	LeastAxis	ClusterShade	HGLRE	GLV	DNUN
Entropy	MajorAxis	ClusterTendency	LRE	HGLZE	DependenceVariance
InterquartileRange	M2DDC	Contrast	LRHGLE	LAE	GLNU
Kurtosis	M2DDR	Correlation	LRHGLE	LAHGE	GLV
Maximum	M2DDS	DifferenceAverage	LGLRE	LALGE	HGLE
Mean	M3DD	DifferenceEntropy	RunEntropy	LGLZE	LDE
MAD	MinorAxis	DifferenceVariance	RLNU	SZNU	LDLGLE
Median	Sphericity	Id	RLNUN	SZNUN	LDHGLE
Range	SurfaceArea	Idm	RunPercentage	SAE	LGLE
RMAD	SVR	Idmn	RunVariance	SAHGE	SDE
RMS	Volume	Idn	SRE	SALGE	SDHGE
TotalEnergy		Imc1	SRHGE	ZoneEntropy	SDLGE
Uniformity		Imc2	SRLGE	ZonePercentage	
Variance		InverseVariance	GLV	ZoneVariance	
Minimum		JointAverage			
Skewness		JointEnergy			
		JointEntropy			
		MaxProbability			
		SumEntropy			
		SumSquares			

GLCM: gray level cooccurrence matrices; GLRLM: gray level run length matrix; GLSZM: gray level size zone matrix; NGTDM: neighborhood gray-tone difference matrix wavelet decompositions.

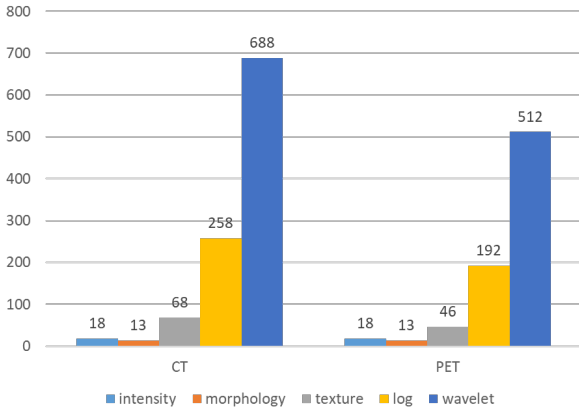


Figure 1. The distribution of extracted features.

Table 2. The parameter settings for features extraction.

Image type	Original	LoG	Wavelet("coif")
Intensity	voxelArrayShift: 1000 padDistance = 10		
GLCM	Distance=1 symmetricalGLCM = True weightingNorm =None	Sigma=1mm Sigma=3mm Sigma=5mm	LLL, LLH, LHL, LHH, HHH, HLL, HLH, HHL
GLRLM	weightingNorm =None		
GLDM(NGLDM)	Distance=1 Gldm_a=0		
GLSZM			
Morphology			

Parameters setting of the Random Forest prediction model

The final prediction model was trained by the Random Forest algorithm with only the three selected important features, and the parameters of the model are listed in **Table 3**.

Table 3. The parameters of RandomForest model.

bootstrap	TRUE
class_weight	None
criterion	'gini'
max_depth	None
max_features	'auto'
max_leaf_nodes	None
min_impurity_decrease	0
min_impurity_split	None
min_samples_leaf	1
min_samples_split	2
min_weight_fraction_leaf	0
n_estimators	100
n_jobs	1
oob_score	FALSE
random_state	24
verbose	0
warm_start	FALSE

Comparison of Skewness features with our selected features

The radiomic study of diffuse large B cell lymphoma [2] reported the diagnostic and prognostic value of the first-order Skewness feature in detecting BMI. However, the Skewness feature was not credible regarding the identification of the BMI in suspected relapsed AL. As recorded in **Table 4**, the Skewness feature along with its variants in cross-validation achieved mean accuracy of 52% (range 34.7%~67.2%) which was much lower than the individual performance of the three features we selected.

Table 4. The individual feature prediction performance of RunEntropy, Kurtosis, SRHGLE and Skewness.

	Features	Mean accuracy
Our selections	Kurtosis_wavelet_LLH.PET	0.708
	RunEntropy_wavlet_LLH.PET	0.727
	SRHGLE_wavelet_LLH.CT	0.767
PET	original_firstorder_Kurtosis.PET	0.437
	original_glrIm_RunEntropy.PET	0.577
	original_glrIm_SRHGLE.PET	0.537
	Skewness_wavelet_LLH.PET	0.487
	Skewness_wavelet_LLL.PET	0.580
	Skewness_wavelet_LHL.PET	0.530
	Skewness_wavelet_LHH.PET	0.479
	Skewness_wavelet_HLL.PET	0.489
	Skewness_wavelet_HLH.PET	0.536
	Skewness_wavelet_HHL.PET	0.563
	Skewness_wavelet_HHH.PET	0.473
	Skewness_log_sigma1.PET	0.502
	Skewness_log_sigma3.PET	0.385
	Skewness_log_sigma5.PET	0.586
	Skewness_original.PET	0.347
CT	Skewness_wavelet_LLH.CT	0.671
	Skewness_wavelet_LLL.CT	0.373
	Skewness_wavelet_LHL.CT	0.626
	Skewness_wavelet_LHH.CT	0.645
	Skewness_wavelet_HLL.CT	0.496
	Skewness_wavelet_HLH.CT	0.420
	Skewness_wavelet_HHL.CT	0.482
	Skewness_wavelet_HHH.CT	0.594
	Skewness_log_sigma1.CT	0.524
	Skewness_log_sigma3.CT	0.466
	Skewness_log_sigma5.CT	0.544
	Skewness_original.CT	0.672
	original_firstorder_Kurtosis.CT	0.411
	original_glrIm_SRHGLE.CT	0.433
	original_glrIm_RunEntropy.CT	0.537

Influence of intra- and inter-observer variability on prediction

We evaluated the influence of both intra-observer and inter-observer variabilities on the performance of our prediction model. The volume overlap error rate (VOE) was used to measure both intra-observer and inter-observer agreement rate where 1 indicating two identical VOIs and 0 indicating no overlap between the VOIs.

Intra-observer variability

To evaluate the influence of intra-observer variability, 16 patients were randomly picked for a second review and adjustment. As shown in **Figure 2**, the mean intra-observer agreement rate with standard deviation was 0.949 ± 0.044 , which led to feature value differences as recorded in **Table 5**. We then performed ten-fold cross-validations on the adjusted patients VOIs. The validation demonstrated that such a minor variability did not pose alteration on prediction decision, justified by 87.5% (14/16) accuracy with two (out of 10) diffuse uptake patient predicted as FPs, which were the identical decision as that in the previous cross-validations.

Inter-observer variability

To evaluate the influence of inter-observer variabilities, we further collected six new patient datasets for independent validation. The six datasets included two diffuse uptake patients, two focal uptake patients and two normal uptake patients. For each new patient, two sets of VOIs were delineated by (1) the same experienced senior operator for the initial 35 patients, and (2) a team of two junior operators. As shown in **Figure 2**, the inter-observer agreement rate was 0.921 ± 0.074 , leading to feature value differences as recorded in **Table 5**. Then, we respectively performed independent validations on the two set of VOIs from the six new patients. The comparison of independent validations results demonstrated that there was no alteration on prediction decision, justified by the same accuracy of 83.3% (5/6) with one (out of two) focal uptake patients incorrectly predicted as FN, while all the diffuse uptake and normal uptake patients were correctly predicted.

In particular, for the two intra- and inter-observer cases with 82.74% and 79.23% as the lowest VOI agreement rates, the model produced consistent predictions.

Further investigation with intentional high variations

To further investigate the influence of higher variations, we randomly picked 13 patients from the initial 35 patients and intentionally exclude various portions of the VOI of the spinal cord to create a new set of VOIs. The agreement rate between these two sets of VOIs was 0.667 ± 0.064 (range 0.509~0.754). The experimental validation showed that the majority of predictions (11 out of 13 patients) remained consistent while two predictions were inverted.

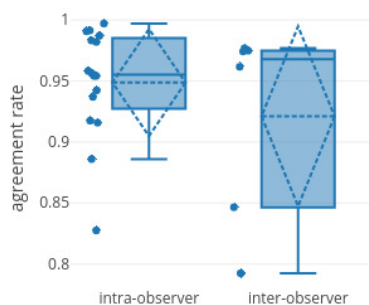


Figure 2. Intra-observer and inter-observer agreement rate based on VOE.

Table 5. Differences on normalized feature values caused by intra-observer and inter-observer variabilities.

	Intra-observer Cases		Inter-observer Cases	
	Mean± SD	Range	Mean± SD	Range
Wavelet-LLH_GLRLM_RunEntropy_PET	0.018±0.036	-0.066~0.092	-0.001±0.069	-0.11~0.1
Wavelet-LLH_firstorder_kurtosis_PET	-0.012±0.475	-0.787~1.624	0.03±0.136	-0.1~0.28
Wavelet-LLH_GLRLM_SRHGLE_CT	-0.003±0.012	-0.007~0.048	-0.006±0.008	-0.02~0

References

1. Zwanenburg A, Leger S, Vallières M, Löck S. Image biomarker standardisation initiative. 2018. arXiv preprint ar Xiv:1612.07003.
2. Aide N, Talbot M, Fruchart C, Damaj G, Lasnon C. Diagnostic and prognostic value of baseline FDG PET/CT skeletal textural features in diffuse large B cell lymphoma. Eur J Nucl Med Mol Imaging. 2018;45:699-711.